

# ON CALIBRATION OF SC SAR IMAGES

P. Corona<sup>(1)</sup>, G. Franceschetti<sup>(2),(3)</sup>, M. Migliaccio<sup>(1)</sup>, V. Pascazio<sup>(1)</sup>

<sup>(1)</sup>I.T.T.O.E.M. - Istituto Univ. Navale - via Acton, 38 - 80133 Napoli (Italy)

<sup>(2)</sup>IRECE-CNR - via Diocleziano, 328 - 80124 Napoli (Italy)

<sup>(3)</sup>Electr. Eng. Dept. - Univ. of Naples - via Claudio, 21 - 80125 Napoli (Italy)

## ABSTRACT

The calibration of SAR images, obtained starting from raw data preserving only the information about sign, and then quantized on two levels, is shown. The experimental results are relative to real and simulated raw data, and show the possibility to calibrate extended and point target.

**Keywords:** Synthetic Aperture Radar (SAR), Coding, Calibration.

## 1. INTRODUCTION

Recently, a new SAR image compression technique has been presented [1]. It involves the signal constituted by the signum of the SAR raw data, hereafter referred as Signum Coded (SC) SAR signal, and for this reason coded at 1 bit. The processing of such SC data by using an SC filter, has also been proposed [2]; because it involves one bit coded two dimensional (2D) sequences, it can be efficiently performed in time domain [3]. Furthermore, quantitative evaluations on the obtained images, regarding the estimation of their grey level distributions [1], of the spatial resolutions [2], and the radiometric resolution [4], have been presented, giving very promising results.

The signum coding of both SAR raw data and filter is an highly non linear operation. The amplitude information carried out by the two signals is totally lost *before* the filtering, but it is totally recovered *after* the data compression, if high level noise is present in addition to the received data [1-2]. The drastic non linearity of the proposed elaboration system, advices, before its practical implementation, to check the possibility of a correct calibration of the obtained images, in order to make such alternative processing fully advantageous with

respect to the (conventional) one of normally quantized data (4-8 bits) and filter (32 bits).

Our attention is mainly focused on relative calibration between two images obtained from SC and conventional quantized data, respectively. Assuming that the latter is exactly calibrated, we calibrate the obtained SC-SAR image. In order to address this purpose we use either simulated or real data. In particular, with reference to simulated data, we use a very powerful SAR raw data simulator [5], especially tailored to the accurate simulation of the surface backscattering coefficient. According to this simulation code we can exactly simulate multifrequency and multipolarized SAR data, also varying system parameters, such as incidence angle, altitude, antenna gain, and so on. Furthermore, we can easily, and exactly, simulate the SAR raw signal received by an arbitrary number of corner reflectors of arbitrary RCS, situated over distributed targets of arbitrary radar backscattering coefficient. This possibility is very attractive from the point of view of image calibration, because we easily check possible critical conditions.

Henceforth such a paper is structured as in the following: part 2 regards the basic concepts underlying the SC SAR theory, part 3 summarizes the SAR raw signal simulator

(SARAS) appropriately tailored and improved to our scopes, in the fourth part we address to the first performed experiments; finally some words are spent to outline future work guidelines.

## 2. SIGNUM CODED SAR THEORY

Let us consider the expression of the instantaneous signal  $\underline{u}(t)$  received on board from the SAR antenna, in its analytical form:

$$\underline{u}(t) = A(t) \exp [j[\omega t + \phi(t)]] + n(t) = u(t) + n(t), \quad (1)$$

constituted by a deterministic  $u(t)$  and a additive random component  $n(t)$ . In Eqn. (1)  $\omega$  is the intermediate frequency, and  $A(t)$  and  $\phi(t)$  are amplitude and phase of the signal envelope. Let us now introduce two new time variables  $t'$  and  $t_n$ , defined by:

$$t' = t - t_n - 2 \frac{R_0}{c}, \quad (2)$$

where  $t_n$  is the discrete variable determined by the pulse repetition frequency,  $R_0$  is the distance between the antenna and the footprint central point, and  $c$  is the speed of light. Substitution of Eqn. (2) in Eqn. (1) leads to the more used two-dimensional expression of the SAR received signal:

$$\underline{u}(t) \rightarrow \underline{u}(x' = wt_n, t'), \quad (3)$$

wherein  $w$  is the platform velocity.

After the signum coded operation, performed separately on real and imaginary parts, we get [3]:

$$\begin{aligned} v(t) &= \text{sgn}[\text{Re}(\underline{u}(t))] + j \text{sgn}[\text{Im}(\underline{u}(t))] = \\ &= \frac{1}{\pi} \sum_{m=1}^{\infty} \epsilon_m j^{m+1} A_m(t) \exp [jm[\omega t + \phi(t)]] = \\ &= \sum_{m=1}^{\infty} v_m(t), \quad m \text{ odd} \end{aligned} \quad (4)$$

$$A_m(t) = \int_{-\infty}^{\infty} \frac{J_m[A(t)\xi]}{\xi} \exp [jn(t)\xi] d\xi, \quad (5)$$

where  $\epsilon_0=1$  and  $\epsilon_m=2$  for  $m \neq 0$  and  $J_m(\cdot)$  is the  $m$ -th order Bessel function. The term characterized by  $m$  even have been omitted, for the reasons just hereafter described.

Let us first assume that the signal is processed, as in a conventional SAR system, by

means of a convolution with an appropriate reference function. The processed signal is given by a coherent weighted superposition of the signal  $v(t)$  at the output of the limiter along a very wide time interval. This operation implies an averaging process over the noise  $n(t)$ , which is nonlinearly coupled with the harmonics of  $v(t)$ , see Eqns. (4) and (5). If we suppose that the noise  $n(t)$  has a gaussian probability distribution  $p(n)$  with zero means and standard deviation  $n_0$ , we can easily evaluate the expected value  $\langle A_m(t) \rangle$  of the  $m$ -th harmonic of the signal [3]. We analyze two possibilities:  $A_m^2(t)/2n_0^2 \gg 1$  and  $A_m^2(t)/2n_0^2 \ll 1$ . In the first one, we get from Eqn. (5):

$$\langle A_m(t) \rangle \cong \frac{2}{m}, \quad m \text{ odd} \quad (6)$$

In the latter case we get:

$$\langle A_m(t) \rangle \cong \sqrt{\frac{2}{\pi}} \frac{1}{\gamma_m} \left( \frac{A(t)}{n_0} \right), \quad m \text{ odd}, \quad (7)$$

with  $\gamma_1=1$ ,  $\gamma_3=-24$ ,  $\gamma_5=640$ , etc. In both cases,  $\langle A_m(t) \rangle = 0$  for  $m$  even; we stress that for this reason the even terms have been already neglected in expansion (4).

We note that the information about the signal amplitude is totally lost when the level of the signal is much greater than the level of the noise; it is preserved in the opposite case, the usual one in SAR applications. A physical explanation of this result is given in Ref. [3].

Hence, if  $A_m^2(t)/2n_0^2 \ll 1$ , the expected signal is composed of the odd harmonics of the original signal, each one with a bandwidth approximately equal to  $mB$ ,  $B$  being the original bandwidth of the modulating signal; furthermore, the level of these harmonics strongly decrease with their order. In particular, the first harmonic is the faithful replica of the SAR raw signal  $u(t)$  via the scaling factor  $\sqrt{2/\pi} n_0$ .

As a second step, let us assume that the same SC operation, as above mentioned, is performed also on the reference function given in its analytical form by:

$$g(t) = B \exp [j[\omega t + \psi(t)]] = g_1(t) + jg_2(t). \quad (8)$$

We separately code its real and imaginary parts, thus getting:

$$\begin{aligned}
h(t) &= \text{sgn}[g_1(t)] + j\text{sgn}[g_2(t)] = \\
&= \frac{2}{\pi} \sum_{s=0}^{\infty} j^{s+1} B_s(t) \exp[j s (\omega t + \psi(t))] \\
&= \sum_{s=0}^{\infty} h_s(t), \quad (9)
\end{aligned}$$

where:

$$B_s(t) = \int_{-\infty}^{\infty} \frac{d\xi}{\xi} J_s(B\xi) = \begin{cases} 1/s & s \text{ odd} \\ 0 & s \text{ even} \end{cases}, \quad (10)$$

because there is no additive noise for the reference signal. Also in this case, the first harmonic of the series (9) is the faithful replica of the reference function via a scaling factor.

Let us now consider the convolution between the SC-SAR signal  $v(t)$  and the SC reference function  $h(t)$ , after the coordinate wrapping (2):

$$\begin{aligned}
v(x',t') \otimes h(x',t') &= \\
&= \sum_{m=1}^{\infty} \sum_{s=1}^{\infty} v_m(x',t') \otimes h_s(x',t'), \\
&\quad m, s \text{ odds}. \quad (11)
\end{aligned}$$

The only significant term of the double summation is the one corresponding to  $m=s=1$  [4], hence:

$$\begin{aligned}
v(x',t') \otimes h(x',t') &\equiv v_1(x',t') \otimes h_1(x',t') = \\
&\frac{4}{\pi^2} \sqrt{\frac{2}{\pi n_0}} u(x',t') \otimes g(x',t') \quad (12)
\end{aligned}$$

The term  $v(x',t') \otimes h(x',t')$  retrieves the conventional SAR image; hence we conclude that the SC operation of both received SAR and reference signals allows to obtain an image that is essentially a replica, but for a scaling factor to the conventional one.

### 3. THE SAR RAW SIGNAL SIMULATOR

Let us introduce now the SAR raw data simulator we use to make a relative calibration between the images processed starting from conventionally and SC quantized data.

Different SAR raw signal simulation schemes are present in literature [5-9], they can be generally casted in a three phases structure. The first phase takes care to the input data phase, the second one is responsible to provide

the electromagnetic behaviour of the scene under survey, the third phase computes the "holographic" signal, i.e. the signal received on board. Within such general scheme the simulation algorithms can be sorted according to specific chances and peculiarities of their three phases. A broad sorting can be made accordingly to the availability of a backscattering model instead of a data base. Different philosophies are involved in the two schemes: the first one reside on a theoretical model, henceforth the simulation code is actually a raw signal simulator, differently the second simulation codes class reside on the chance to exploit opportune data bases. In this paragraph we recall the SAR raw signal simulator hereafter employed; it can be sorted in the first class even if is able to manage real data [5-10]. Such simulator has been modularly improved in order to incorporate the chance to simulate the desired corner reflectors. Hence, in this paragraph we describe the SAR raw signal simulator SARAS [5], employed in this work.

The holographic signal  $u(\cdot)$ , i.e. the signal received on board before any processing, can be casted, for a stationary scene, in the following form:

$$u(x',r') = \iint dx dr \gamma(x,r) g(x'-x, r'-r; x,r) \quad (13)$$

wherein  $g(\cdot)$  is the unit response function and  $\gamma(\cdot)$  the backscattering coefficient (i.e. the ratio between the backscattered and incident electrical field phasors); reference is made to the fixed orthogonal coordinate systems depicted in Fig.1. We note that the sensor is mounted on a vector flying with constant velocity along the azimuth line ( $x$ -axis) and regularly emits short modulated pulses in the side looking direction (SLAR).

As already stated a SARAS keypoint is the convenient evaluation of the reflectivity map; this is accomplished by means of an electromagnetic model rather than exploiting a data base, then SARAS is a SAR raw signal simulator able to generate the corresponding holographic signal  $u(\cdot)$  pertaining an extended three dimensional scene [5,10].

The considered model is based on the Kirchhoff solution to the backscattered field and it requires, on one side, the topographic description of the relief as well as its permittivity and permeability behaviour [5,10]. Then a statistical description of the scene is due [5]. On the other side the radar description is necessary.

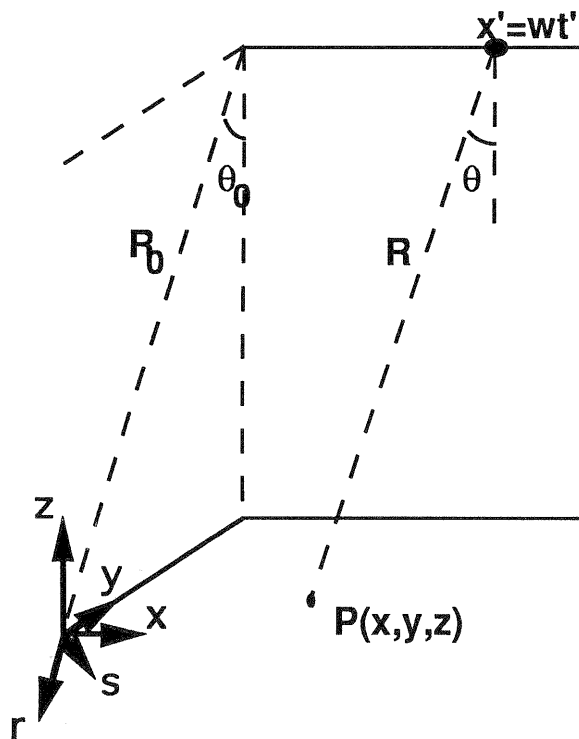


Fig. 1: Reference systems

The model employs a piecewise planar approximation of the terrain relief; i.e. the surface is modelled by means of planar facets large in terms of the incident wavelength, so to apply the former Kirchhoff solution to the problem.

Letting an incident local plane wave over the single facet, we get [5]:

$$E_s = \frac{j k \exp(-jkR)}{4 \pi R} E_0 (\underline{\underline{I}} - \hat{\underline{\underline{k}}}\hat{\underline{\underline{k}}}) \int_A F(a,b,c) \exp [2j \underline{\underline{k}} \cdot \underline{\underline{\rho}}] dA \quad (14)$$

where  $E_0$  is the incident field amplitude,  $\underline{\underline{k}}$  the corresponding vector wavenumber,  $\underline{\underline{I}}$  the unitary matrix, (a,b,c) are the components of the normal vector to the facet A and finally  $\underline{\underline{\rho}}$  the pointing vector describing the integration domain. The vector  $F(\cdot)$  is a function depending on the Fresnel coefficients pertaining to the facet, hence it takes care of polarization capabilities. Its expression, in the radar reference system sketched in Fig.1, is evaluated in Ref.[5].

Once the reflectivity map has been determined, computation of Eqn.(13) can be accomplished through efficient two-dimensional FFT codes. In addition analytical evaluation of

the filter function has been performed. A complete discussion regarding this conceptual aspect can be found in Refs.[5,11]. Finally Eqn. (13) can be written in the following form:

$$U(\xi, \eta) = \Gamma(\xi, \eta) G(\xi, \eta) \quad (15)$$

where  $(\xi, \eta)$  are Fourier conjugate variables to  $(x, r)$  and capital letters indicate the FT of corresponding space domain function.

Such general simulation scheme has been improved by the chance to simulate prescribed corner reflectors backscattering coefficients over an extended scene; incidentally we remind the capabilities to correctly simulate speckle [5].

Let us finally note the great importance of a SAR simulator in developing inverse techniques, such a tool must therefore correctly built to create canonical and reliable scenarios.

As graphical summary of the SAR raw signal simulator (SARAS) a pictorial block scheme of it is shown in Fig. 2.

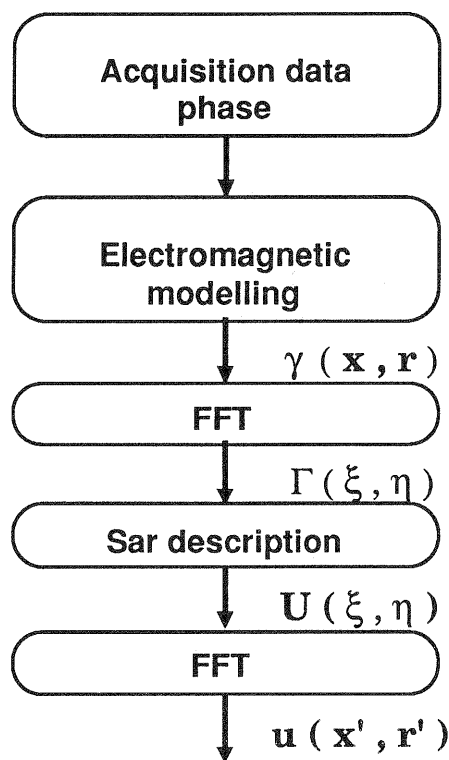


Fig. 2: Simulator block scheme

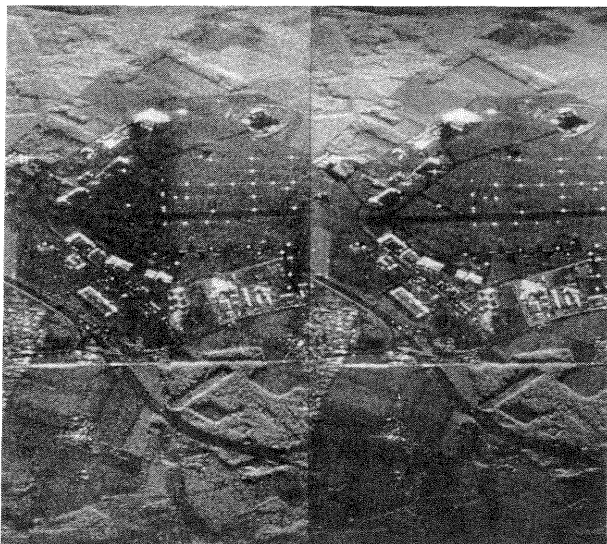
#### 4. EXPERIMENTS

Let us proceed with the discussion about calibration of real and simulated processed images.

Starting from real SAR images, the results of the processing of SC and conventionally quantized raw data, relative to the DLR E-SAR

airborne mission made on the area of Oberpfaffenhofen airport (1989), are shown in Figs. 3(a) and 3(b), respectively. The images appear to be very similar; from a quantitative point of view, many tests can be done. First of all, the grey level statistical distribution evaluated on image zones that appear to have uniform backscattering characteristics, by means of Kolmogorov statistical test, shows that in both processing schemes (conventional and SC) the distribution is of Rayleigh kind [1]. Furthermore, the radiometric resolution, i.e. the system capability to resolve intensity levels, appear to be almost equal in both cases [4].

The purpose of this paper is to check the possibility to have a relative calibration between the two images, i.e. the system capability to have a one to one correspondence between the images pixel levels. If we suppose that the image processed starting conventionally quantized data is already calibrated, the above mentioned one to one correspondence ensure us that the calibration of the SC-SAR images is possible, in other word, it is possible to assign to their pixel levels the corresponding values of the backscattering coefficient.



(a)

(b)

Fig. 3: SAR images processed starting by SC(a) and conventional data (b)

The correspondence between the pixel level of the two images of Fig. 3, can be evaluated by means of the joint probability distribution  $p(\cdot, \cdot)$  of their intensity levels  $I$  and  $I_{sc}$ . The ideal case occurs when the joint distribution have values different from zero only when  $I=I_{sc}$ , otherwise have values equal to zero. This joint distribution

for the eight lower levels, (taken by 255 total levels) of the two images is shown in Fig. 4. The origin of the figure is in the upper left corner and the horizontal axis corresponds to the  $I$  values while the vertical one to the  $I_{sc}$  ones. We can read the figure as follows: let us consider a slice cut of  $p(I, I_{sc})$  for a fixed  $I$  value (vertical cut). The curve that comes out is the SC grey level distribution  $p(I_{sc} | I)$  and shows that the mean value is equal to  $I$ , and the standard deviation is small, so that the  $I_{sc}$  values are concentrated around  $I$ . In Fig. 5 the slice cut relative to  $I=2$  is shown and proves the general result above discussed.

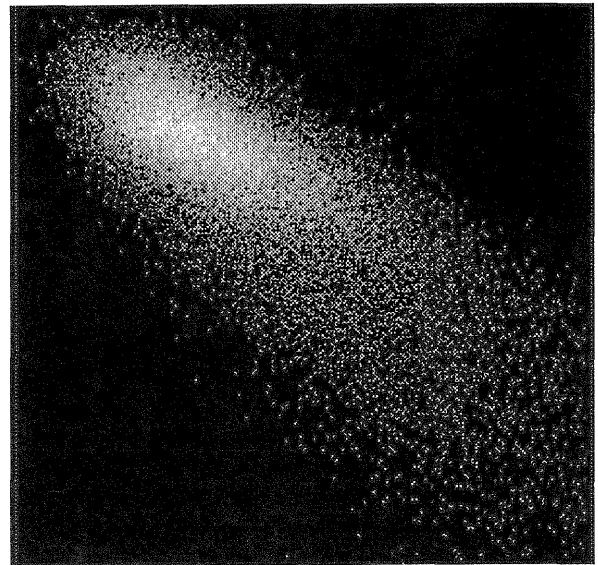


Fig. 4: Joint probability distribution of the levels of the two images of Fig. 3

The proposed experimental scheme can be applied to simulated data. In fact, in calibration issues a complete control of the scene is desired and this can be performed by means of such simulated data. Some examples have been performed. On the line to build a proper setup the SAR raw signal simulator has been adjusted to include the routine which simulates the corner reflectors. Hence a composite flat terrain, composed by rough areas made by materials with different complex permittivity, deterministic zone and different corner reflectors, has been simulated and the corresponding traditional processing [11] has been generated.

In order to properly generate raw signal  $u(\cdot)$  additive noise was inserted in the

simulation chain. The results relative to corner reflectors of arbitrary RCS positioned over different grounds, provides a joint probability distribution in good agreement with the one found in the real images case.

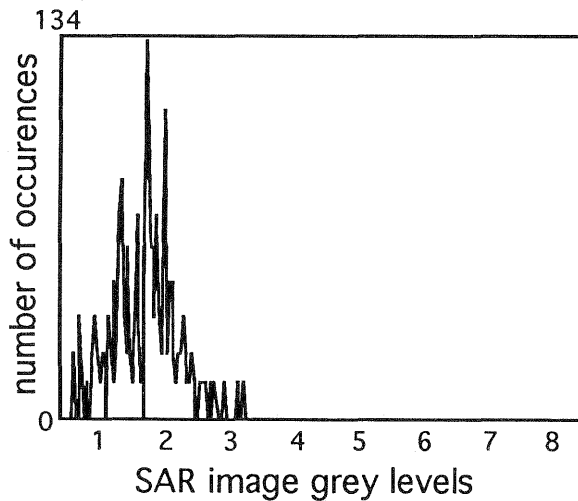


Fig. 5: Vertical slice cut of Fig. 4

#### REFERENCES

- [1] G. Franceschetti, V. Pascazio, G. Schirinzi, "Processing of Signum Coded SAR Signal: Theory and Experiments", *Proc. IEE, Pt. F*, **138**, pp. 192-198, 1991.
- [2] G. Alberti, G. Franceschetti, V. Pascazio, G. Schirinzi, "Time Domain Convolution of One Bit Coded Radar Signals", *Proc. IEE, Pt. F*, **138**, pp. 438-444, 1991.
- [3] G. Franceschetti, A. Mazzeo, N. Mazzocca, V. Pascazio, G. Schirinzi, "Time Domain Processing of SAR Data in Real Time", *Proc. IGARSS'91*, Helsinki (Finland), pp. 283-286, 1991.
- [4] A. Brancaccio, G. Franceschetti, V. Pascazio, G. Schirinzi, "Quality Measurements on SC-SAR Images", *Proc. IGARSS'92.*, Houston (USA), 1992.
- [5] G. Franceschetti, M. Migliaccio, D. Riccio, G. Schirinzi, "SARAS: a SAR Raw Signal Simulator", *IEEE Trans. Geos. Rem. Sens.*, **GE-30**, pp. 101-112, 1992.
- [6] F.W.Leberl, **Radargrammetric Image Processing**, Norwood,MA, Artech House, 1990.
- [7] J.C.Holtzman, V.S.Frost, J.L.Abbott, V.H.Kaupp, "Radar Image Simulation", *IEEE Trans. Geosci. Rem. Sensi* **GE-16**, pp. 296-303, 1978.
- [8] T.K.Pike, "SARSIM: A SAR System Simulation Model", *DFVLR Mitteilung*, 1985.
- [9] D.G.Corr, "SAR Simulation for Land Use", in *Proceedings of the EARSeL workshop on SAR Simulation Models*, Capri (Naples), Italy, 1988.
- [10] G.Franceschetti, M.Migliaccio, D.Riccio, "Microwave Imaging: A Synthetic Aperture Radar Simulator of Extended Three Dimensional Real Ground Sites", *to be submitted*.
- [11] G.Franceschetti and G.Schirinzi, "A SAR processor based on two- dimensional FFT codes", *IEEE Trans. Aerosp. Electron. Syst.*, **AES-26**, pp. 356-366, 1990.